Influence of pump pulse structure on a transient collisionally pumped Ni-like Ag x-ray laser

K. A. Janulewicz* and P. V. Nickles
Max Born Institute, Max-Born-Strasse 2A, D-12489 Berlin, Germany

R. E. King and G. J. Pert
Department of Physics, University of York, Heslington, YO10 5DD York, United Kingdom
(Received 8 December 2003; published 13 July 2004)

Results of numerical simulations on a Ni-like silver x-ray laser pumped by a single picosecond laser pulse are presented. Since the mechanisms responsible for the significant reduction in the pump energy are not well understood, the results of theoretical simulations with emphasis on the plasma kinetics and dynamics in a Ni-like Ag x-ray laser are presented and referred to the experimental data. Special attention has been paid to the influence of the pump pulse shape and length on the gain and its duration. It was found that a low-level pulse pedestal being an integral part of the leading edge of the pump pulse is very beneficial to the pump energy reduction. The thermal cooling process has been identified as the mechanism strongly contributing to gain termination if a low-energy single-profile laser pulse with the width of a few picoseconds is used in the pump process.

DOI: 10.1103/PhysRevA.70.013804 PACS number(s): 42.55.Vc, 42.50.Ar, 52.50.Jm, 42.25.Kb

I. INTRODUCTION

Much effort in x-ray laser development has been put into downsizing. As dimensions of the laser driver determine the size of the whole system, the compactness of the pump systems becomes a decisive factor in achieving laboratory scale x-ray lasers (XRL). The first attempts to build such a system concentrated on the optical-field-ionized plasma as an active medium. Using subpicosecond pulses of defined polarization with an energy of a few hundred millijoules, lasing in H-like lithium at 13.5 nm [1,2] and Pd-like xenon at 41.8 nm [3] was achieved. However, recent progress in the development of the OFI lasers [4,5] has not altered the relatively low practicability of this scheme in competition with high harmonics, especially at wavelengths above 30 nm [6]. Demonstration of the collisional pump scheme with transient inversion [7] and the progress observed in the development of the pump laser technology have enabled large strides to be made towards the goal of practical tabletop XRLs. Application of the pump scheme referred to above to moderate-Z elements (Mo, Pd, Ag, Sn) ionized to the stages of the Ni-like isoelectronic sequence [8–10] has shown that, in principle, it is possible to saturate the x-ray laser with the emission wavelength between 10 and 20 nm with the energy significantly lower than 10 J [8,10–12]. Moreover, the application of a longitudinal (along the axis of the plasma column) pump arrangement with a subpicosecond laser pulse has permitted laser action in a Ni-like molybdenum system at 18.9 nm with a pump energy of only 150 mJ [13]. Ni-like ions are especially interesting as lasants for efficient XRLs due to the more beneficial scaling of the pump energy towards shorter wavelengths. The advantage of the transient inversion scheme relies on the separation of the ionization and heating processes in the plasma of the active medium. This facilitates tailoring of the plasma heating onset to the required plasma ionization stage. Decomposition of the pump pulse into two separate, adjustable delayed pulses with different lengths, proposed and experimentally demonstrated in Refs. [7,14], has removed the temporal mismatch between both processes existing in the case of a single pump pulse. Two pump pulses are applied in the pump scheme with the transient inversion. The first, long nano- or subnanosecond pulse, creates the plasma with the required ionization stage, and the following high intensity pulse, usually with pico- or subpicosecond duration, rapidly heats the medium and generates conditions beneficial to the collisonal excitation. However, it was found that a slight increase in the short pulse duration to a few picoseconds results in reduction in the pump energy [15]. The last result was the starting point for application of a single pump pulse formed in such a way that a low-level background has created an underionized preplasma, and the following high-intensity part of the pulse has further ionized and rapidly heated it [12]. Saturation of Ni-like Ag XRL at 13.9 nm with only 3 J of the pump energy has been achieved with this pump method. The most important aspect of this result is the identification of a pump parameter set which allows for the utilization of commercial non-CPA (chirped-pulse-amplification) lasers with high repetition rate as x-ray laser drivers. With current technology it has proved possible to construct a laser driver with an energy of only 1 J in a pulse length of $\sim$6 ps at a repetition rate up to 1 kHz [16].

The present paper attempts to explain the basic physics responsible for working of this pump scheme, and is organized as follows. After a short introductory part, the model used in the simulations and the numerical code are briefly described. Then, the results of simulations, starting with the input data similar to those reported in the proof-of-principle experiment [11,12], are presented. Some of the prospects for further development are also discussed.

*Electronic address: kaj@mbi-berlin.de

II. PLASMA KINETICS MODELING

The complexity of the phenomena observed during the XRL experiments requires theoretical support, mostly in the form of sophisticated and dedicated numerical codes. Numerical modeling helps us to understand the physics behind the measurable parameters of the active medium. Although not all the effects observed are fully reproducible by the simulations, the elucidation of the trends in the changes resulting from the variation of the input parameters can help us to understand and control the experimental results. This latter position is adopted in respect to the results presented below. There have been a few attempts to model transient Ni-like collisional x-ray lasers of moderate-Z elements such as palladium, silver, or molybdenum, but to date all have failed to accurately reproduce the experimental results [17,18] at the level achieved for the Ne-like isoelectronic sequence [19].

A. Theoretical model

In the numerical simulations the 1.5-D hydrodynamics and atomic physics code EHYBRID developed in York has been applied [20]. The EHYBRID code has been successfully used to reproduce experimental results for ions from the Ne-like isoelectronic sequence if the incident energy is reduced by a factor of 2 from that actually used in the experiment. However, this factor depends on the particular laser characteristics, and also on the absorption nonlinearity. It may, therefore, be expected to be reduced at the low intensities which are present in our pump pulse parameters. Although the most appropriate value of this factor is unknown, we have set the correction factor to 1 for the background pulse and 2 for the short intense pulse in the simulations presented here. With this proviso, all values are set equal to those from the experiment demonstrating saturation in Ni-like Ag x-ray laser with a single picosecond laser pump pulse and the pump energy of 3 J in a focal spot of width 80 μm over a length of 6 mm [11,12].

An important uncertainty in this simulation is the nature of the ablation process during the low-intensity background heating phase. The ablation process is determined by the low-level background with the width between a few hundred picoseconds and a few nanoseconds, and is responsible for the subsequent beam propagation and the laser output. However, the dominant mechanism of an underdriven ablation process with a fluence of a few joules per square centimeter (in our case $\sim 4\ \mathrm{J/cm^2}$) is still unclear. At these intensities the material should be described by the full equation of state including solid-liquid-gas phase transitions for accurate results. A preliminary calculation using a simplified ChartD model was carried out, but was not satisfactory. The aim of this work was exploratory and qualitative. Rather than seeking to generate accurate quantitative data, it was decided to use the common approximation of the ideal gas equation of state (EOS) with a full treatment of the ionization development, despite its limitations.

A combination of two separate pulses with regulated amplitudes, lengths, and partly shapes (flatness of the low-level pedestal) has been used to model the single-profile picosecond laser pulse applied in the experiment. The preforming part of the pump pulse used in the modeling includes optionally a background with a defined rise time, a flat-topped pedestal with the same total length, and a linearly increasing ramp (Fig. 1). Unless an alternative is indicated, the energy of the pump pulses was kept constant during the shape variations. The full width at half maximum (FWHM) of the pulse completes the pump pulse characteristics. The notation of the pulse description presented for the picosecond pulse in Fig. 1 is valid also for any other pulse. The main, short part of the pump pulse (assumed to be always Gaussian) was usually switched on at the maximum of the background. Generally, it was accepted that the total pump energy was about 2.6 J and its part included in the low-level pedestal would be no larger than 20 mJ. These values were used during the parameter variations as a reference, and corresponded reasonably accurately to the typical experimental conditions.

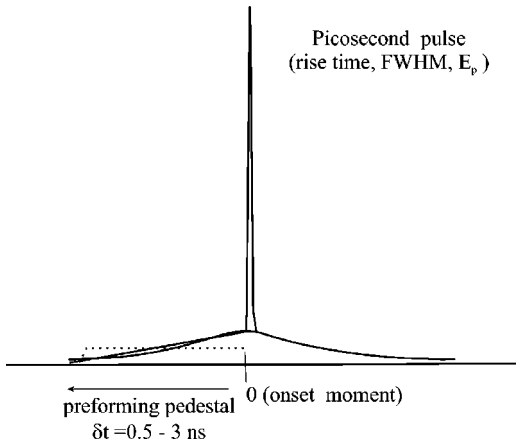

FIG. 1. Sketch of the pump pulse structure with three different forms of the background used in modeling—a Gaussian ramp, linear ramp, and flat-topped pulse. The picosecond laser pulse is described according to the notation applied to characterize the pump laser pulses.

The output data from EHYBRID can be postprocessed with a 3D ray-tracing code, giving full characteristics of the output beam including its near- and far-field images as well as a set of ray-averaged parameters related to a uniform medium with corresponding output characteristics. The code can trace the short-wavelength output at a steady-state gain, i.e., it corresponds rather to the case of matched traveling wave pumping. However, it can give the output at different times of the gain development. The collisional excitation rates by the monopole collisions have been obtained by processing of the atomic data produced by Cowan's atomic code [21].

B. Results

The question regarding the identification of the physics responsible for lasing in the transient Ni-like scheme pumped with only a single, low-energy (E_p as low as 0.9 J) picosecond pump laser pulse is the most important one which can be investigated by the simulation results. The answer to this question can be facilitated by the analysis of the most important parameters such as the local gain coefficient, plasma density, average ionization stage Z^*, and the electron

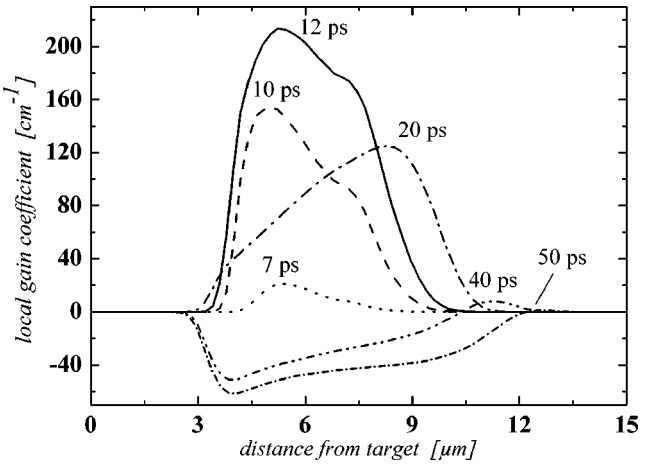

FIG. 2. Distribution of the local gain coefficient as a function of the distance from the target for a Gaussian pedestal and different times delayed with respect to the short pulse onset. The pump pulse is described in the notation of Fig. 1 by (2 ns, 2 ns, 20 mJ); (3 ps, 6 ps, 2.6 J).

temperature T_e. The short pump pulse component was simulated by a 6-ps pulse (FWHM) with the rise time optionally of 3 or 6 ps. Some calculations are also presented, which were carried out using shorter ($\sim$1 ps) and stronger main pump laser pulses, as used in our initial experiments. It should be noted that the total length of the Gaussian pump pulses, as were used here in EHYBRID, is equal to the doubled rise time; hence, any change of the rise time has consequences for the absorption process.

Figure 2 presents the spatial profile of the local gain coefficient in the direction normal to the target surface (expansion direction) at different times delayed relative to the onset of the short part of the laser pump pulse. The plot presented in Fig. 2 corresponds to the pulse energy of 2.6 J and the pump pulse structure described according to the convention presented in Fig. 1 as (2 ns, 2 ns, 20 mJ); (3 ps, 6 ps, 2.6 J). This plot reveals the first important aspect of the specified pump method. In contrast to typical experiments, where it was assumed that only overionization is responsible for gain termination, we have noticed that plasma cooling by thermal conduction into the bulk material contributes strongly to the reduction in gain and hence also affects the gain lifetime. It is clearly seen that the gain spatial profile progressively attenuates and flattens on the target side of the medium. A cold absorptive wave (in the x-ray domain) canceling the gain spreads out over the active medium into the plasma plume. As a consequence, the reduced (partly also by overionization) gain shifts its maximum in the same direction. The gain duration (FWHM) and the gain decay constant for the same pump pulse as in Fig. 2 have been estimated as equal to 12.5 ps and 9.8 ps^{-1}, respectively. The first value suggests that the output signal would propagate slightly more than 4 mm during the gain lifetime and corresponds to the saturation length observed in the experiment.

The temporal history of the gain for different values of both the preforming and heating pump pulses is shown in Fig. 3. It can be concluded from the plots presented there that the long and flattened pulses are more beneficial for increasing the gain duration. Additionally, the active medium volume increases as longer pedestals support a longer expansion. Higher but shorter gain could be obtained with a shorter background in the form of a ramp (amplitude increasing slowly with time). An increase in the background energy increases the gain duration.

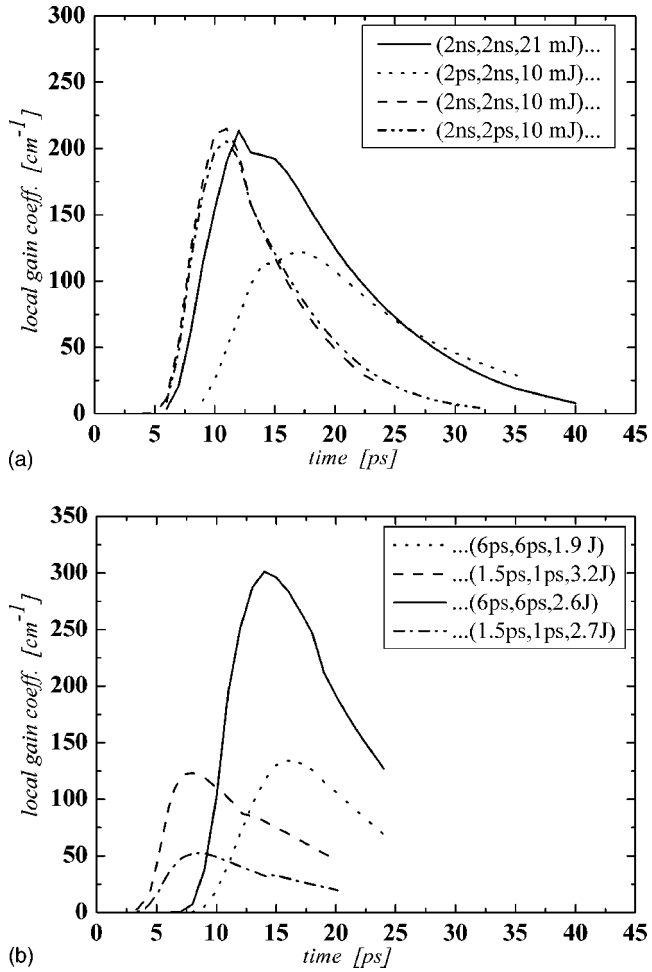

FIG. 3. The time history of the local gain coefficient for (a) different background pulse parameters combined with an intense component in the form (3 ps, 6 ps, 2.6 J) and (b) different intense components of the pump pulse preceded by the background pulse (2 ns, 2 ns, 20 mJ).

In contrast, increase in the energy of the short pulse shortens the gain lifetime, as this accelerates the ionization process and thus facilitates the overionization. Figure 3 shows also that the time duration of the intense part of the pulse affects the gain characteristics even more strongly. Decreasing the short pulse from 6 to 1 ps (FWHM) accompanied by an increase in the energy of more than 65% results in a gain reduction of more than 50% under the same plasma preforming conditions. Furthermore, maintaining the pump energy unchanged, while the intense part of the pump pulse was shortened, yet again halved the maximum gain [dash-dot line in Fig. 3(b)].

The temperature of the electrons differs from that of the ions in the two-fluid model applied in the code. The radial distribution of the electron temperature in the plasma plume

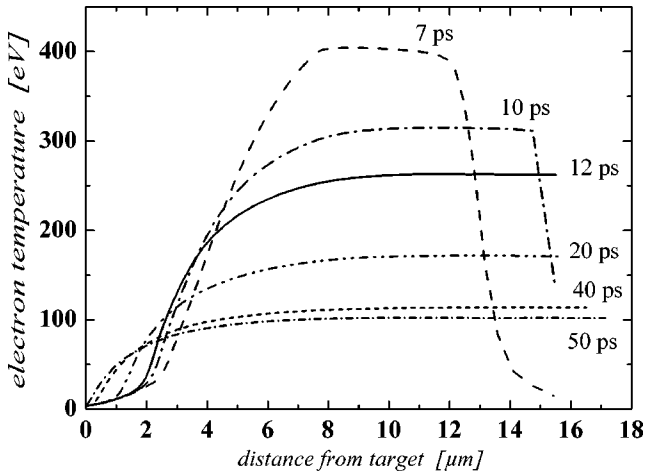

FIG. 4. Distribution of the electron temperature vs the distance to the target for different times delayed relative to the short pulse onset. Pump pulse: (2 ns, 2 ns, 20 mJ); (3 ps, 6 ps, 2.6 J).

at the same pump conditions as in Fig. 2 is shown in Fig. 4. The temperature reaches the maximum of about 400 eV quite early, and then drops rapidly but within a significantly larger volume of the active medium. The electron energy at this temperature allows the plasma to efficiently excite the upper laser level, as allowed by the atomic data for Ni-like Mo, Pd, and Ag ions at temperatures above 250–300 eV. The significant negative gain (absorption) observed as a result of cooling is dominantly caused by a very high plasma density present in the regions with a reduced electron temperature (Fig. 5). It is interesting that the electron density distribution, despite its very high absolute value, does not show extremely steep density gradients and, even more, some sort of a temporally stable plateau exists at the high gain area (Fig. 5). This density distribution is responsible for the strong absorption of the pump radiation observed in the medium, and this effect compensates mainly a low initial average ionization stage ($Z^* \leqslant 3$) at the short pulse onset. From these results, we observe two key features of this system.

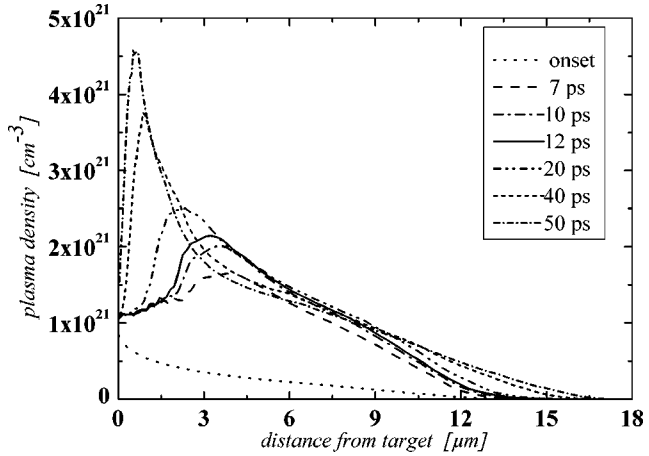

FIG. 5. Distribution of the plasma density vs the distance to the target for different delays respective to the short pulse onset moment. (2 ns, 2 ns, 20 mJ); (3 ps, 6 ps, 2.6 J).

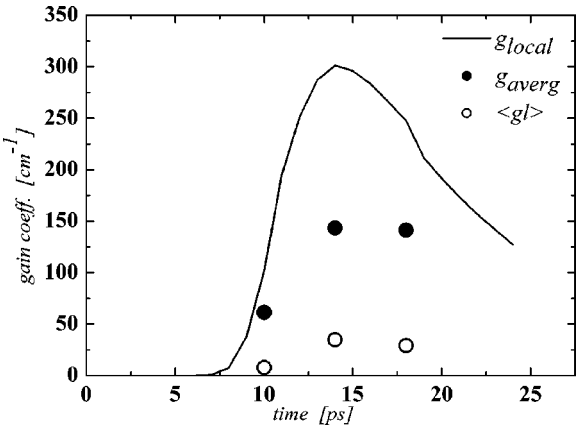

FIG. 6. The time history of the local and ray-averaged (dots) gain coefficients as well as that of the averaged gain-length product. The pump pulse: (2 ns, 2 ns, 20 mJ); (6 ps, 6 ps, 2.4 J).

(1) A plume of sufficient density to allow strong absorption, but low mass to permit high temperatures to be developed with relatively small energy inputs.

(2) The development of a stable, low gradient density profile capable of supporting the x-ray laser beam against refractive loss.

In the standard double-pulse scheme the ionization was typically completed before the arrival of the main short and intense pulse. This required significantly higher energy level of a nanosecond preforming pulse. The requirement for a rapid creation of the abundance of Ni-like ions and the following fast excitation process have caused a strong trend towards shortening of the main part of the pump pulse. It has resulted in shortening of the gain lifetime due to fast overionization, but at the same time a significant part of the energy available in the pump process was directed to nonusable ionic species. The low-level background input intensity applied in the single-pulse pump scheme delivers a dense, low-ionized active plasma, and near completion of the ionization process occurs parallel to collisional excitation during the extended picosecond part of the pump pulse. Cooling is a relatively slow process and the excitation at high density is very efficient. Thus, the gain achieves both a high value and a reasonably long-lived character.

The density gradients strongly influence the XRL output by refraction. The ray-averaged gain (used in the uniform active medium representation) is shown in Fig. 6, and represents the gain seen along a weighted (by its output intensity) ray path. The value of the averaged gain coefficient is about 50% of the spatial peak value. However, both the ray-averaged gain and the averaged gain length product decrease more slowly than the peak gain. This effect is caused by the outward shift in time of the gain peak (Fig. 2) into regions of lower density where refraction is weaker. At early times the rays are more strongly refracted through a range of gain, and therefore sample both the high and low gain parts of the spatial distribution. In contrast, later in time the dominant rays are refracted less, sample the peak gain more strongly, and are expected to be more distinct at the inherent speed of the excitation wave. Thus, it would support the unusually long output x-ray pulses measured in the experiment [11].

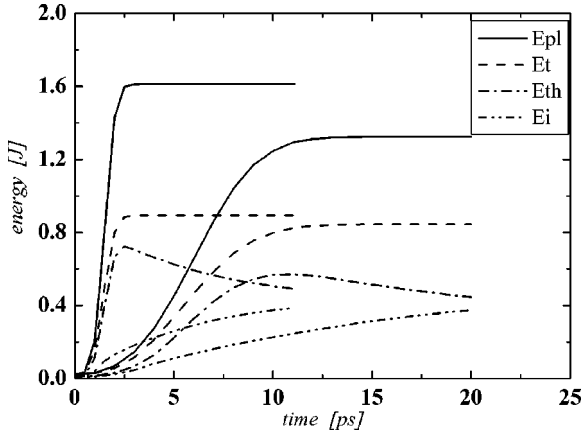

FIG. 7. The time history of the energy deposition in the plasma under two different irradiation conditions. The group of the curves on the left side of the plot within the time gap between 0 and 12 ps corresponds to the pulse in form (2 ns, 2 ns, 20 mJ); (1.5 ps, 1 ps, 3.2 J) and the other one to the pulse described by (2 ns, 2 ns, 20 mJ); (6 ps, 6 ps, 2.6 J). E_{pl} represents laser energy delivered (solid); E_t is total energy absorbed (dashed); E_{th} is thermal energy (chain); and E_i is ionization energy (dash+double-dot).

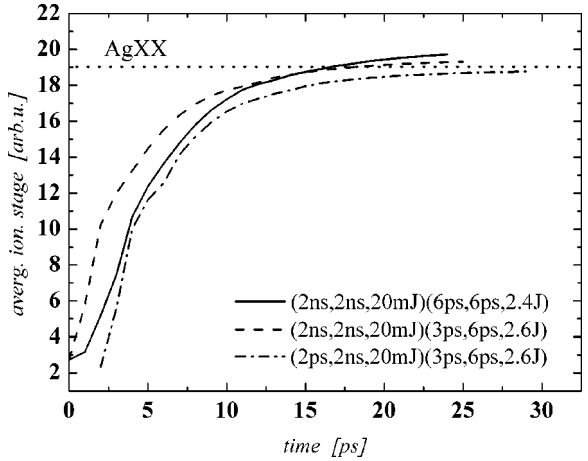

FIG. 8. The time history of the maximum ionization stage in the plasma irradiated with the pulse of different temporal forms.

We note, however, the apparent disagreement between the values of the gain and the gain-length product (plasma length 6 mm), and also that the difference between these values increases with time. In fact, both effects are a consequence of the strong refraction, which will be more clearly illustrated later, whereby the dominant rays have a strongly curved path and sample a wide range of gain in the plasma.

The advantage of the extended heating pulse is clearly seen in Fig. 7. Despite the reduction in the delivered pump energy of more than 30%, the total energy deposited in the plasma is nearly unchanged (dashed lines). Higher plasma temperatures achieved on a shorter time scale cannot be beneficial to gain, as the ionization level at the onset of the heating pulse component is too low and is only slightly changed within the interval until the maximum electron temperature T_{emax} has been achieved. By applying longer pump pulses this relation becomes much more favorable for the energy deposition. It should be stressed again that increase in the energy of the longer pump pulse boosts the gain but shortens its lifetime and reduces its volume. Shortening of the gain duration is understandable in this case as the relative contribution of overionization to the gain termination process starts to dominate, and that of thermal cooling is correspondingly reduced. When the intense part of the pump pulse is lengthened to 6 ps, the absorption region resulting from the cold plasma does not appear after a few tens of picoseconds, even though the cooling influence on the spatial gain distribution is visible.

Figure 8 shows the temporal history of the average ionization stage in the cases of three different laser pump pulses. The ionization level corresponding to Ni-like Ag (Ag^{+19}) is marked in the figure. The solid line illustrates the changes occurring during a strong pumping pulse with rise time extended to 6 ps. The other two curves correspond to pumping with a more steeply rising short component (3-ps rise time), and one of them (the chain line) demonstrates influence of the flat-topped (in contrast to Gaussian) pulse as the preforming pedestal. The differences in approaching the required ionization stage are clearly seen. The intense heating part of the pump pulse is decisive for the ionization process. Even if energetically weaker, and in the initial phase less efficient, the extended pulse accelerates the overionization (solid line in Fig. 8). On the other hand, the flat-topped pedestal pulse leaves the preplasma in a lower ionization stage and the identical short part of the pump pulse is no longer able to ionize silver to the stage of Ni-like isoelectronic sequence (compare the dashed and chain lines in Fig. 8). This behavior also helps to explain some points in the earlier discussion on the gain termination mechanism.

Near-field images have been obtained in the experiment using the second (opposite to the spectrograph input) face of the plasma column. This was possible as traveling wave pumping was not implemented. The modeled near-field images are shown in Fig. 9 at the times corresponding to the gain maximum (14 ps after the onset of the heating pulse) and when the peak gain value had been reduced to less than 50% of its maximum value (22 ps). The experimental beam profile seen in Fig. 10 is strongly dependent on the pump parameters of the laser, and its curvature increased with increasing pump energy: indeed, the experiments show a strong dependence of the beam shape in the near field on the pump parameters of the laser. We see in Fig. 9 that with the moderately long-lived gain there is a noticeable movement of the most intense part of the beam in the expansion direction. Since the time interval between both snapshots is only 8 ps, it must be expected that the experimental near-field images have been smeared and do not give reliable information on the exact dimensions of the active volume. From the simulation data we observe that this effect seems to be caused by a shift of the gain area in the medium rather than any hydrodynamic movement. In fact, this is a result of the refraction occurring in the plasma which gives rise to deflections of $\sim$10 mrad. The dominant ray (i.e., that with the maximum gain length) has a curved path with its perihelion approximately at the midpoint of the plasma length. Since the position of the output rays is strongly determined by refraction and therefore by the density gradient, small errors

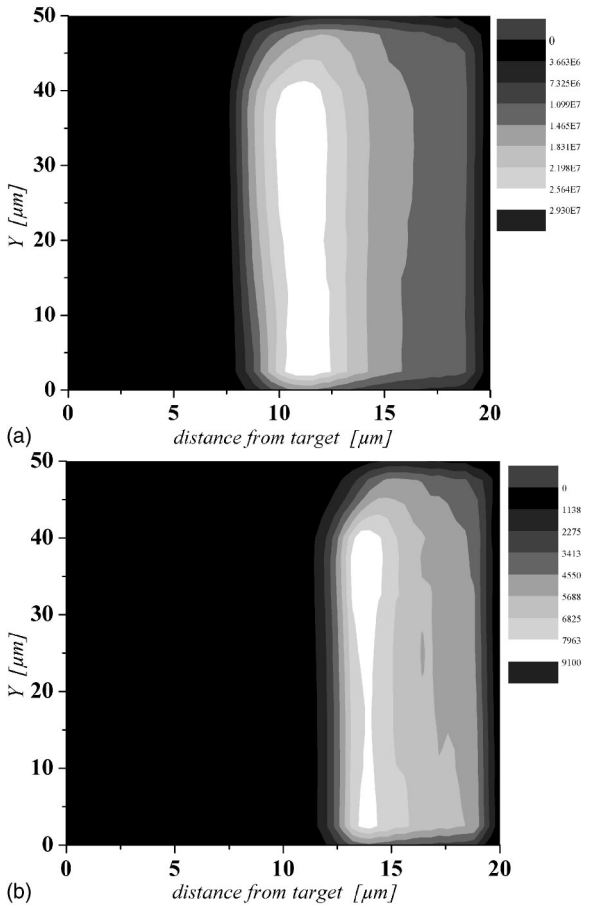

FIG. 9. Near-field patterns obtained by ray tracing: (a) 14 ps (maximum gain) and (b) 22 ps after the onset of the short component. The plots show only the upper half of the symmetric image.

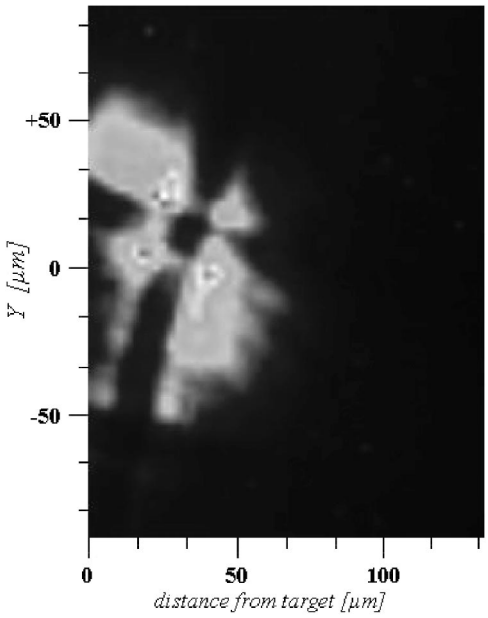

FIG. 10. The near-field image of the beam registered in the experiment with the pump pulse of ~5 ps width and energy of 1.45 J. The cross seen in the image center comes from the mesh supporting the Al filter. The vertical axis corresponds to the position of the target surface which was determined by separate shots with crossed wires positioned 3–4 mm from the target edge.

in the latter will make a marked difference in both the position and the shape of the output pattern. The behavior of the output signal in the presence of a refraction limited saturated output was investigated in Ref. [22]. In this case there will be a family of similar rays traversing the plasma, each displaced along the axis and in the absence of absorption leaving the plasma with similar energy, but displaced upward. In particular, depending on the position of the perihelia, the output can be narrow in the direction perpendicular to the target surface (as seen in the simulation) or wide (as in the experiment). A shift of less than 1 mm is sufficient to account for the experimental result. This effect is not normally observed as in conventional systems the gain has a greater spatial extent and lies further out.

III. DISCUSSION

Modeling of the plasma created by a "shaped" low-energy picosecond pulse has actually confirmed suitability of this pump method for collisional x-ray lasers working with Ni-like moderate-Z elements. Thus, the simulation results presented support in many aspects of the qualitative interpretation of the experimental results reported in Refs. [11,12]. It is found that the low-intensity ablation process is critical in controlling the x-ray laser process. This occurs in the following important ways:

(i) A low-mass, cold, and relatively dense plume is evaporated from the target surface. But, this plume with small spatial extent strongly absorbs the main pulse.

(ii) Due to the low plume mass a high electron temperature is generated which leads to rapid ionization and strong collisional excitation of the upper laser level.

(iii) Due to the small spatial extent of the plasma and the density gradient, the laser output is refraction limited (in these simulations over a distance of ~6 mm).

However, the experimental results are poorly reproduced quantitatively. This is not entirely surprising, since, as noted, the low-intensity ablation is poorly described. However, the profile of the ablated plasma plume before the onset of the main heating pulse is a key determinant of the output process through refraction. It is unlikely that the basic form of this plasma has been incorrectly modeled, since that is determined by the conservation laws inherent in the fluid description. However, quantitative details such as, for example, the mass of the plasma will not be correct. The failure to accurately model the near-field patterns observed experimentally almost certainly originates from this approximation. Bearing these limitations in mind, the experimental near-field spot of $\lesssim$50-μm width displaced ~30 μm from the target surface (recorded 3.5 mm from the target edge) corresponds very well with the spot position (~35 μm) determined with the modeled value of a ~10-mrad deflection angle. It is also in reasonable agreement with the displacement of 8–15 μm at the end of the plasma column determined by ray tracing.

It was found that the scheme is extremely sensitive to the shape and energy of both components of the laser pump

pulse. In many cases the background pulse can be provided by the pedestal normally present with CPA pulses by relaxing the normal stringent conditions used to ensure its removal. However, unless a sophisticated pulse shaping technology is developed and installed, the background can only be controlled over a limited range.

IV. CONCLUSIONS

The pump scheme described in the paper shows some similarity to the prepulse technique combining low-energy prepulses with long main (the width about 100 ps) pump pulses [23]. The similarity relies on a low-level prepulse with energy reduced to 0.1%–10% of the main pulse energy. In the scheme described in the present paper the pedestal (background) energy was equal to ~1% of the total energy. However, in this scheme the main pumping pulse is significantly shorter and this dramatically affects the x-ray laser parameters, especially the gain factor and pump energy level.

The numerical modeling of the Ni-like Ag soft x-ray laser emitting at 13.9 nm and pumped by a single picosecond laser pulse with energy lower than 3 J has been performed. In spite of some inconsistencies between the theoretical and experimental results discussed in the paper, the results obtained are very helpful in understanding some of the basic phenomena responsible for efficient lasing in this pump scheme. The simulations have demonstrated essential suitability of this pump method for elements from the Ni-like isoelectronic sequence and have given useful support for the results of the proof-of-principle experiment [11].

ACKNOWLEDGMENTS

We acknowledge R.D. Cowan from LANL for making his code available and help in getting it to work, as well as P. Mandelbaum from Hebrew University of Jerusalem for comprehensive Ag data, generated with HULLAC, used as a reference.

[1] Y. Nagata, K. Midorikawa, S. Kubodera, M. Obara, H. Tashiro, and K. Toyoda, Phys. Rev. Lett. **71**, 3774 (1993).
[2] D. V. Korobkin, C. H. Nam, S. Suckewer, and A. Goltsov, Phys. Rev. Lett. **77**, 5206 (1996).
[3] B. E. Lemoff, G. Y. Yin, C. L. Gordon, III, C. P. J. Barty, and S. E. Harris, Phys. Rev. Lett. **74**, 1574 (1995).
[4] S. Sebban *et al.*, Phys. Rev. Lett. **86**, 3004 (2001).
[5] A. Butler *et al.*, Phys. Rev. Lett. **91**, 205001 (2003).
[6] K. A. Janulewicz, A. Lucianetti, G. Priebe, and P. V. Nickles, X-Ray Spectrom. (to be published).
[7] P. V. Nickles, V. N. Shlyaptsev, M. Kalachnikov, M. Schnürer, I. Will, and W. Sandner, Phys. Rev. Lett. **78**, 2748 (1997).
[8] J. Dunn, A. L. Osterheld, R. Shepherd, W. E. White, V. N. Shlyaptsev, and R. E. Stewart, Phys. Rev. Lett. **80**, 2825 (1998).
[9] J. Dunn, Y. Li, A. L. Osterheld, J. Nilsen, J. R. Hunter, and V. N. Shlyaptsev, Phys. Rev. Lett. **84**, 4834 (2000).
[10] J. Dunn, J. Nilsen, A. L. Osterheld, Y. Li, and V. N. Shlyaptsev, Opt. Lett. **24**, 101 (1999).
[11] K. A. Janulewicz, A. Lucianetti, G. Priebe, W. Sandner, and P. V. Nickles, in *Proceedings of 8th International Conference on X-Ray Lasers, Aspen 2002*, edited by J. J. Rocca, J. Dunn, and S. Suckewer, AIP Conf. Proc. No. 641 (AIP, Melville, NY, 2002), p. 26.
[12] K. A. Janulewicz, A. Lucianetti, G. Priebe, W. Sandner, and P. V. Nickles, Phys. Rev. A **68**, 051802 (2003).
[13] T. Ozaki, R. A. Ganeev, A. Ishizawa, T. Kanai, and H. Kuroda, Phys. Rev. Lett. **89**, 253902 (2002).
[14] S. Maxon *et al.*, Phys. Rev. Lett. **70**, 2285 (1993).
[15] J. Dunn, A. L. Osterheld, J. Nilsen, J. R. Hunter, Y. Li, A. Ya. Faenov, T. A. Pikuz, and V. N. Shlyaptsev, in X-Ray Lasers 2000, Proceedings of the 7th IXRLC in St. Malo, France, 2000, edited by G. Jamelot, C. Moeller, and A. Klisnick [J. Phys. IV **11**, Pr2-19 (2000)].
[16] P. V. Nickles, K. A. Janulewicz, G. Priebe, A. Lucianetti, R. Krömer, A.-K. Gerlitzke, and W. Sandner, in Soft X-Ray Lasers and Applications V, edited by E. E. Fill and S. Suckewer [Proc. SPIE **5197**, 29 (2003)].
[17] J. Nilsen, J. Dunn, R. F. Smith, and T. W. Barbee, Jr., J. Opt. Soc. Am. B **20**, 191 (2003).
[18] J. Kuba *et al.*, J. Opt. Soc. Am. B **20**, 208 (2003).
[19] R. E. King *et al.*, Phys. Rev. A **64**, 053810 (2001).
[20] G. J. Pert, J. Fluid Mech. **131**, 401 (1983).
[21] R. D. Cowan, *The Theory of Atomic Structure and Spectra* (University of California Press, Berkeley, 1981).
[22] G. J. Pert, in *Proceedings of 8th International Conference on X-Ray Lasers, Aspen 2002* (Ref. [11]), p. 279.
[23] J. Nilsen *et al.*, Report UCRL-JC-112704, Livermore, CA (1993).